INL/CON-17-41768-Revision-0

Novel Short-Circuit Detection in Li-ion Battery Architectures

Sergiy V. Sazhin, Eric J. Dufek, David K. Jamison

October 2017

The INL is a U.S. Department of Energy National Laboratory
operated by Battelle Energy Alliance

INL/CON-17-41768-Revision-0

Novel Short-Circuit Detection in Li-ion Battery Architectures

Sergiy V. Sazhin, Eric J. Dufek, David K. Jamison

October 2017

Idaho National Laboratory
Idaho Falls, Idaho 83415

http://www.inl.gov

Prepared for the
U.S. Department of Energy
Office of Energy Efficiency and Renewable Energy
Under DOE Idaho Operations Office
Contract DE-AC07-05ID14517

Novel Short-Circuit Detection in Li-ion Battery Architectures

S. V. Sazhin, E. J. Dufek, D. K. Jamison

Department of Energy Storage & Advanced Vehicles, Idaho National Laboratory,
Idaho Falls, Idaho 83415, USA

Industry and the battery research community don't have accurate and affordable methods to predict catastrophic battery failures. Recently we published a new method of early detection of nascent internal shorts that are precursors to catastrophic failure. This present work was performed to determine the methods short detection capability within battery architectures consisting of two parallel strings with up to four cells in the string. It was found that detection sensitivity is a function of the number of healthy versus compromised cells in the architecture and placement of the measuring device. The method allows one to locate shorted cells without disconnecting cells or loads from the battery architecture.

Introduction

As energy storage devices become more important in the management of the world's power supply, safeguarding large battery assemblies from catastrophic failure (CF) has become a top priority. Although lithium-ion batteries are found in a wide array of applications, from mobile phones to commercial airliners, the continued expansion of lithium-ion batteries is hindered by safety, durability, and reliability concerns. Li-ion chemistry consists of flammable materials and may be unsafe without proper safeguard. One cause of CF is the internal short-circuit (SC), which causes thermal runaway and ignition of the flammable materials. The present industry trend is to push for higher power and energy density by several approaches, including the application of thinner separators. Thinner separators, higher energy densities, larger battery sizes, complex battery architectures and sheer numbers of battery products, entering the consumer space, increase the likelihood of CF incidence. Unfortunately, no fast industry-accepted method to forecast a CF exists.

The methods of detection of internal SC and measurement of self-discharge have been discussed in literature for decades (1-9). However, for broad industry adoption, a method should be fast, accurate, non-destructive, and applicable to any cell chemistry or battery design. Recently, we proposed a new fast approach to the detection of Li-ion cell soft SC's far before a CF occurs (10-12). This approach differs from earlier work by addressing industry needs in more detail. The approach demonstrated high precision during development and was validated on single 18650 Li-ion cells. Electric drive vehicles and other field applications with battery architectures consisting of numerous serial-parallel connected cells require fast detection of cell soft short-circuits. The purpose of present work is to further investigate capabilities of the SC detection method and determine its usefulness when applied to more complicated battery architectures.

Such information is vitally important for the acceptance of this method in the diagnosis of battery state-of-health in a variety of field applications.

Experimental

Brief description of the method

The soft short-circuit detection approach is based on the application of a constant voltage (V_{TEST}) to a short-circuited cell or battery at a slight discharge overvoltage from fractions of mV to several mV, depending on the battery system and desired speed of SC detection. Discharge overvoltage is the difference between the initial OCV or voltage under load (V_{INI}) and V_{TEST}. It will also be referenced as an undervoltage. During this slight discharge polarization, which causes minimal battery disturbance, the response signal (measured current) transitions from an initial high negative value to a stabilized positive value through a current zero crossing point (CZCP), Figure 1.

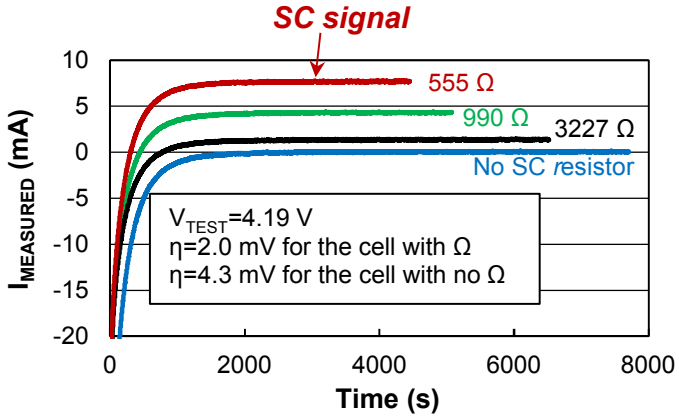

Figure 1. Current response under V_{TEST}=const<V_{INI} for a single cell (11).

A stabilized, positive current under the potentiostatic V_{TEST} condition is the metric for SC detection. This SC current, I_{SC}, compensates self-discharge (SD) caused by SC. The current response is the same whether the soft short is internal or external, therefore, we used external resistors of different resistivity to mimic internal soft short-circuits. The rationale for using external resistors for validation of the method for different battery architectures was to achieve reproducible and controllable results in a safe manner. External resistors dissipate Joule heat outside the cell eliminating possible cell thermal runaway. There is no reproducible procedure that can create the specific internal short-circuit resistance values needed to validate this method. Creation of internal shorts increases the possibility of thermal runaway.

Healthy 18650 cells, in the case where no external SC resistor is attached, generate over time the negligible positive stabilized current in the typical range from 5 to 30 µA. This is the near zero current in Figure 1 that compensates for genuine SD caused by electrochemical and chemical side reactions. The small value of this current, I_{GEN_SD}, doesn't influence practical discrimination of shorts. As can be seen from Figure 1, lower-resistance shorts result in a higher SC current. The SC current value is not a function of

the undervoltage value or battery chemistry and design. When I_{GEN_SD} is very small, SC current is predominately a function of the short-circuit resistance where, $I_{SC} = V_{TEST}/R_{SC}$. For different undervoltages the equilibration time varies. However, the same SC current value is finally achieved. In order to minimize the time of detection, a smaller undervoltage value should be used based on cell chemistry and design. The method philosophy, definitions and differences vs. prior art are discussed in more detail in previous publications (10, 11). Analysis of test results in this paper is based on the SC current metric.

Varying battery architecture

Multiple Sanyo UR18650SAX high-power lithium-ion cells, with a minimum rated capacity of 1.25Ah, were combined in varying battery architectures to determine the capabilities of the method. Architectures with up to two strings and up to four cells per string were studied. Sensitivity of soft short-circuit detection was studied as a function of the number of short-circuited cell(s) in the battery architecture, their position within the string and the position of the potentiostat. For comparison consistency, resistors with a nominal resistivity of 500 Ω were used to generate the soft shorts.

A Solatron SI 1287 Electrochemical Interface with Solatron SI 1260 Impedance/gain-phase analyzer was used for the studies. The Solartron SI 1287 Electrochemical Interface potentiostat was connected in varying ways: to a single short-circuited cell, to a single not-short-circuited cell, to a short-circuited and not-short-circuited cell in the string, to a single or dual string containing different numbers of short-circuited and not-short-circuited cells. Some single and dual string experiments had a known constant load connected to the battery architecture in order to estimate the capability of detecting a soft short without decoupling the load. A 10% tolerance 3 kΩ resistor was used as a load. Experiments with known external resistive loads were designed to mimic field scenarios. In the field, load examples are battery-control circuitry, such as a battery management system (BMS), or vehicle equipment connected to the battery. It is assumed that a vehicle is parked, not driven, during this type of diagnostics.

In order to compare capabilities of the potentiostatic method with Electrochemical Impedance Spectroscopy (EIS), impedance studies were performed on a single shorted cell and strings consisting of one shorted cell and up to 3 healthy cells versus identical architectures of all healthy cells. The impedance studies were done for the cells at 10% state-of-charge (SOC) at OCV immediately after potentiostatic polarization at V_{TEST}. The frequency range of interest in this work was 0.01 Hz to 100 kHz.

The Solartron potentiostat provides DC polarization within a voltage range of ±14.5 V with a maximum resolution of 100 μV. This voltage range allows testing the string(s) of four cells at 10% SOC (V_{TEST} = 3.533 V per cell) or the string(s) of three cells at 90% SOC (V_{TEST} =4.091 V per cell). An undervoltage of 10 mV per cell was used for all testing conditions in this study.

All experiments were done with the cells in thermal equilibrium inside an environmental chamber (ESPEC, model BTU-133). The temperature was maintained at 30°C during testing. For all experiments, Solartron leads were physically bolted to the cells' tabs to

ensure a reliable, reproducible connection. To reduce resistances between battery architecture cells, AWG 14 jumper wiring was used with lengths of no more than four inches. Short-circuit and load resistors were connected outside the chamber.

Method of data processing

During the applied undervoltage process, current recording was split into two intervals using specific potentiostat settings. The first interval was from the time polarization started at a maximum negative current to the time current reduces to negative 5 mA. The second was from negative 5 mA to the positive stabilized current passing through CZCP. This was done to utilize the higher accuracy of the potentiostat, reduce nose in the smaller current ranges and provide a smooth transition through the CZCP. Only portions of current from negative 5 mA to the positive stabilized current are presented in the graphs for simplicity of illustration in this paper. For consistency of comparison of I_{SC}, obtained from varying battery configurations, a special data processing procedure was used. I_{SC} was calculated as an average over the time interval from 5400 to 9000 seconds after the CZCP. The CZCP is a legitimate reference due to the fact that by the time the CZCP occurs, all testing scenario cells have almost arrived at the same state of equilibration with the potentiostat. The small difference relates only to final compensation of SD caused by soft shorts (11).

Results and Discussion

Understanding signal strength evolution is required in order to detect short-circuits in battery architectures. Factors effecting signal strength are the number of short-circuited cells, number of healthy cells, potentiostat position within the battery architecture, and the presence of a battery load. It is also necessary to understand measurements given no disconnection of cell(s) or the battery load from the battery architecture.

Evolution of short-circuit current in strings with one shorted cell and a varying number of healthy cells

A schematic representation of the studied string circuits at 10% SOC and I_{SC} evolution at 10% and 90% SOC is illustrated in Figure 2.

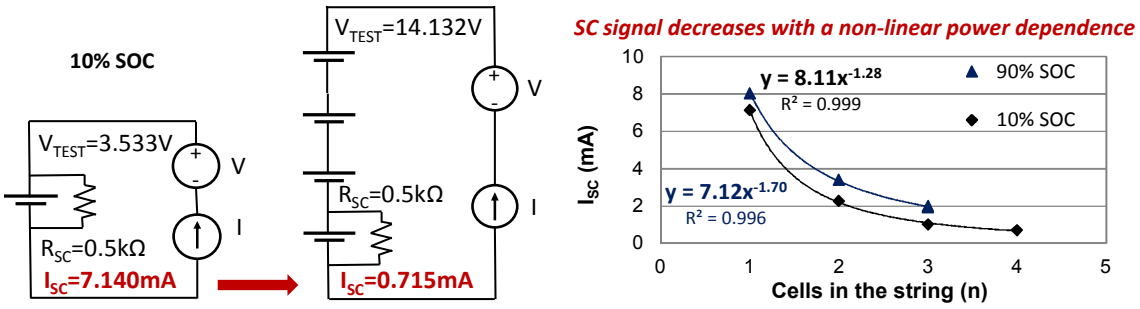

Figure 2. I_{SC} evolution for strings containing one short-circuited cell. 3-cell string-90% SOC. 4-cell string-10% SOC.

The circuits at 90% SOC are not shown in the figure due to their similarity to 10% SOC circuits. For these experiments the potentiostat was connected to the strings. The V_{TEST}=const voltages were adjusted to the length of the string and SOC. The 3.533 V was used for a single cell, 7.066 V for 2-cell, 10.596 V for 3-cell and 14.133 V for a 4-cell string at 10% SOC. At 90% SOC, the 4.091 V was used for a single cell, 8.180 V for 2-cell, 12.274 V for 3-cell string. As more healthy cells are added to the short-circuited cell, the I_{SC} signal decreases with nonlinear power dependences. At the 10% SOC condition, the power coefficient is minus 1.70. For 90% SOC it is lower in absolute value (-1.28). At higher SOCs amplitude of the signal is higher. Therefore, suggesting tests should be conducted at higher SOCs. Short detection at the highest SOCs makes sense considering nascent dendrite shorts form at highest SOCs during charging.

Adding a healthy string in parallel to a string containing one shorted cell doesn't reduce detection sensitivity for the two string combination, Figure 3. A healthy string doesn't generate additional current. For a battery architecture containing one equivalent short in two strings, the signal doubles, Figure 3. This behavior enhances short detectability. When the string with I_{SC} current is found, measurements can be done on string segments and finally on each cell in the compromised segment.

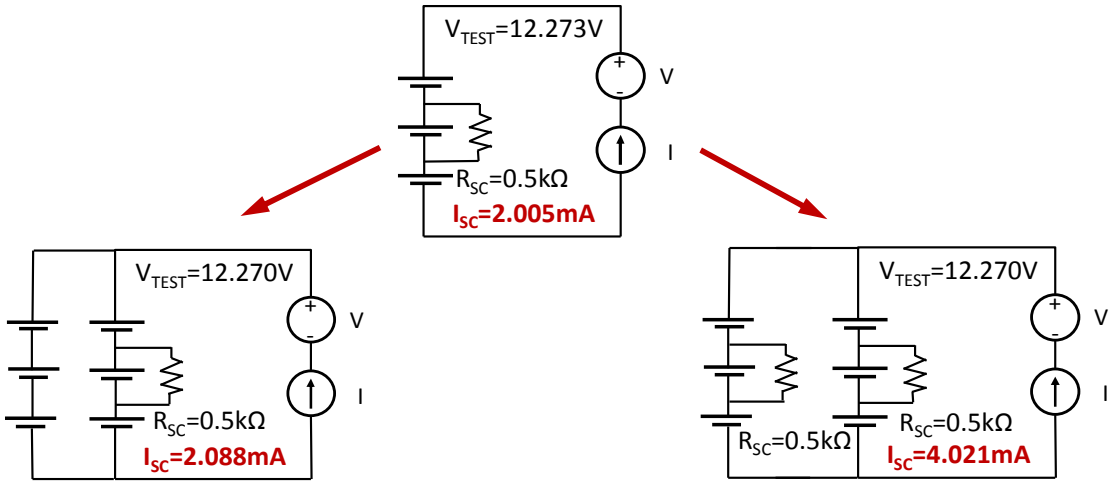

Figure 3. I_{SC} evolution with the addition of a parallel string at 90% SOC.

Evolution of short-circuit current in strings with increasing number of shorted cells

A schematic representation of 4-cell strings with different numbers of short-circuited cells at 10% SOC and I_{SC} evolution at 10% and 90% SOC is illustrated in Figure 4. The 3-cell circuits at 90% SOC are not shown in the figure due to similarity to 10% SOC circuits. The V_{TEST}=const voltages were adjusted to the SOC. At a 10% SOC the string of four cells was at a voltage of 14.132 V and at a 90% SOC the string of three cells was at a voltage of 12.273 V. As more shorted cells are added to the string, the I_{SC} signal increases with a nonlinear power dependency. It is interesting that the absolute value of the power coefficients in the dependencies are the same for studies with one shorted cell in a string of varying numbers of healthy cells compared to a string of four cells with varying numbers of shorts (compare graphs in Figures 2 and 4). However, the signs of the coefficients are different. Another observation is that strings with all cells shorted have an

I_{SC} signal equivalent to the single cell circuit (close to 8 mA at 90% SOC and 7 mA at 10% SOC).

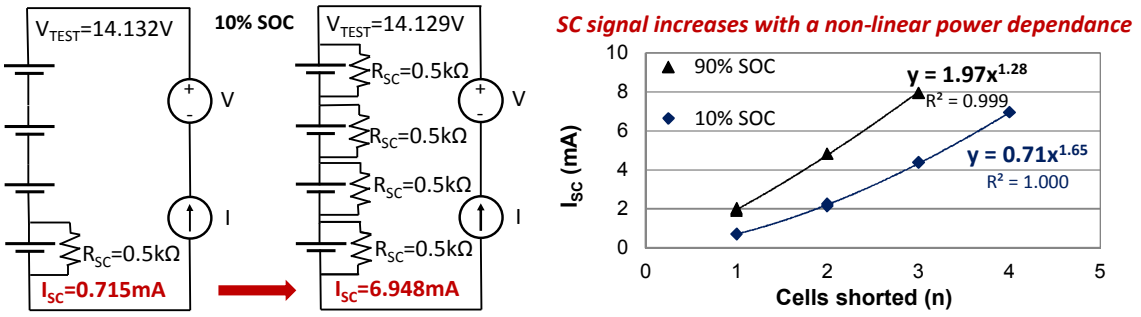

Figure 4. I_{SC} evolution in 3-cell and 4-cell strings with the number of short-circuited cells.

Short-circuit detection with battery architecture under constant load

In a majority of configurations the battery architecture is permanently connected to the load. An example of a primary battery load is the EV engine. An example of a mild secondary load is controlling circuitry such as the BMS or vehicle auxiliary equipment. Checking battery status with the primary load connected has limitations due to fast changes in the battery SOC and the high currents associated with that change. When large currents are running through the battery architecture to a primary load one cannot discriminate the small I_{SC} signal from the large current.

Secondary or auxiliary loads change the SOC significantly slower and discharge currents may be in a range closer to I_{SC} currents providing more opportunity for diagnostics. To determine the method capabilities under mild load conditions, the circuitry of Figure 5 was studied. In this case a constant load of 3 kOhm was connected to a string consisted of one shorted cell. The potentiostat was attached across a string of three series connected cells.

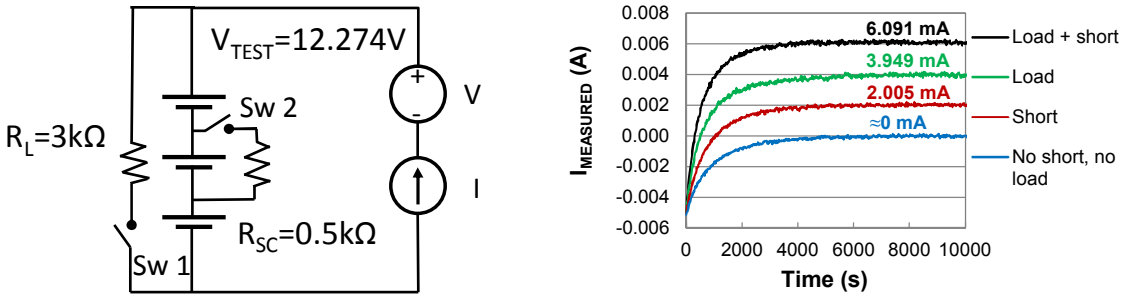

Figure 5. I_{SC} measurement under a known constant load at 90% SOC.

Depending on what shorting switches are closed, different values of stabilized positive currents are detected, Figure 5. It is important to mention that mild auxiliary loading produces a current response (I_L) with a similar appearance to the soft short

current response. In this experiment I_L is 3.949 mA. This number can also be derived from the equation [1].

$$I_L = V_{TEST}/R_L \quad [1]$$

For industry adoption it is important to have short detection capability without disconnecting the battery from the load. In this experiment, when both switches are closed, the currents for all loads sum up, I_{SC+L}=6.091 mA. If the load resistance is known, the current related to a soft short may be determined by the equation [2].

$$I_{SC} = I_{MEASURED\_POSITIVE\_STABILIZED} - V_{TEST}/R_L \quad [2]$$

In other words, if the measured positive stabilized current exceeds the calculated load current, there is a shorted cell in the string. This experiment clearly shows that decoupling the load from the battery architecture is not required to find a problem. For systems equipped with a BMS, the BMS continuously monitors load current.

Detection of a shorted cell in a string under load

A practical question is, whether it is possible to find a shorted cell in a string under load without disconnecting the cell from the string? To answer this question two electrical circuits were studied, Figure 6. In the circuit on the left, the potentiostat is connected to the shorted cell. In the circuit on the right, the potentiostat connection is to a healthy cell.

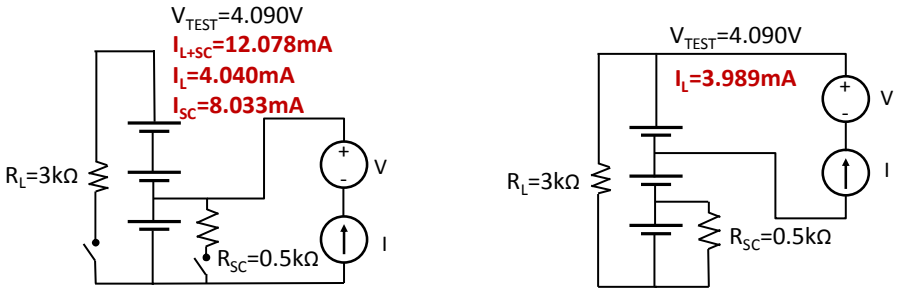

Figure 6. I_{SC} measurement for the cell within the string at 90% SOC.

When both switches on the left circuit are closed, the sum of the load and short currents is detected at 12.078 mA. The short current is 8.033 mA and the load current is 4.040 mA. Therefore, if the measured current during diagnostics exceeds the known load current, then the short current can be calculated using equation [3].

$$I_{SC} = I_{MEASURED\_POSITIVE\_STABILIZED} - V_{STRING}/R_L \quad [3]$$

In the circuit to the right, Figure 6, for a healthy cell within a string under load the only detected current is the load current, I_L. This means that if measured current doesn't exceed calculated load current the cell is healthy. These studies demonstrate that cell disconnection from the string is not required to find a shorted cell.

To determine a batteries' state–of-health, full battery architectures can first be checked for SC problems. Then problematic strings and string segments can be found. Finally, faulty cell(s) within the string segment can be identified.

Impedance measurements

There are some opinions in the battery community that an impedance technique may be used for short-circuit detection. To investigate the ability of impedance measurement to detect short-circuits, typical Nyquist plots were obtained immediately after potantiostatic polarization at V_{TEST} for a single cell and strings of two, three and four cells, Figure 7. Two scenarios are compared for each string configuration. In the first scenario, the strings consisted of only healthy, not shorted cells. In the second one, a single shorted cell was used separately and within the strings. As can be seen, the plots in Figure 7 are almost identical and don't discriminate shorted conditions. The explanation for low sensitivity of the impedance technique is simple. For example, with the studied single cell condition, the 0.5 kΩ short is connected in parallel with a relatively low cell ohmic resistance (0.02 Ω at $Z''=0$ in the graph of Figure 7). For this parallel connection the total impedance is 0.0199992 Ω. The difference in ohmic resistance for the shorted and not shorted condition is only $8 \cdot 10^{-7}$ Ω. This small difference is not detectable by using the impedance technique. Early detection requires that nascent shorts be detected while short impedances are fairly high (even greater than 0.5 kΩ) in order to catch the condition well before CF. Detection capability will be much worse than discussed here.

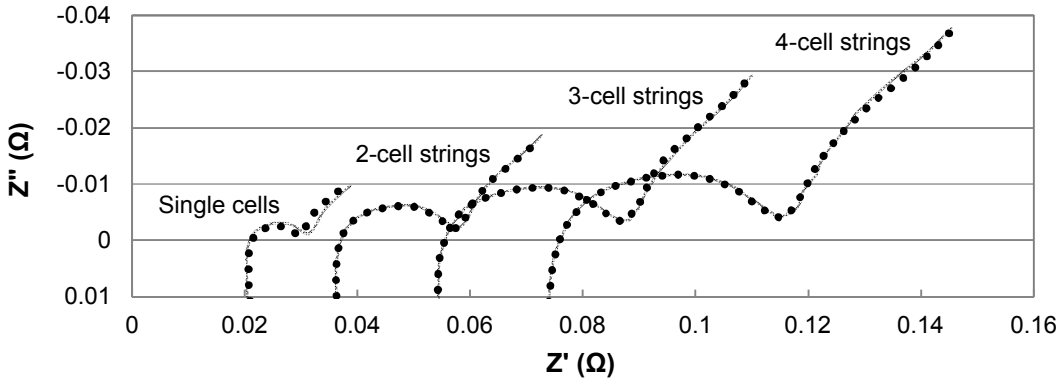

Figure 7. Nyquist plots for the single cell and the strings at 10% SOC. Dotted line — healthy cells. Solid line — shorted single cell and the strings consisting of one shorted cell.

Conclusions

In response to a need to eliminate catastrophic failures in large battery architectures, capabilities of our new method of short-circuit detection were studied. Our method uses self-discharge current or short-circuit current as a metric for short-circuit detection. This metric was derived by new effective approach (10, 11). Battery architectures consisting of two parallel strings with up to four cells in the string were used to understand the detection capability of the method. Soft short-circuit currents were accurately detected at

the cell level, single string level and dual string level when a cell or battery architecture is under constant load or rest conditions. When a soft short within the battery architecture is detected, additional measurements can discriminate the fault to a string and faulty cell(s) position within the string. Disconnection of the cell or the load from battery architecture is not required to conduct the test. The measured amplitude of soft short-circuit current depends on where the potentiostat is connected within the battery architecture. The signal strength is proportional to the number of soft shorts in the battery architecture. Increased cell count of shorted cells in a string increases the SC signal with a non-linear power dependence. Increased cell count of healthy cells in a string decreases SC signal with a non-linear power dependence. Addition of a parallel string with healthy cells does not affect detection sensitivity. There is no decrease in detection capability at the cell level if the cell is within a string under load. If a potentiostat is connected to a healthy not-short-circuited cell in a single string battery architecture, containing other short-circuited cells and a load, only load current is detected. No short-circuit current is running in the diagnostic circuit when connected to a healthy cell.

This patent-pending method is accurate, fast, non-invasive, applicable to any battery chemistry or design and capable of detecting nascent shorts (12). The method is compatible with battery management systems for monitoring battery state-of-health at any time or state-of-charge.

The method appears to be a universal diagnostic tool capable of monitoring a battery throughout its life span. Initially, it can be used for the detection of faulty cells under production, and then it can be applied at the beginning of life during initial characterization (mapping) of battery performance. It can also be used for periodic state-of-health checks during the operational life of the battery in comparison to the beginning of life. When the battery reaches the end of life, which is 80% of state-of-charge for electric-drive vehicle applications, it may be repurposed for secondary use in residential or industrial storage. This is a critical time for checking for shorts to avoid problems in larger battery architectures.

Technology, based on this method, can be used for electric-drive vehicles, stationary energy storage, military, aeronautic, portable electronic devices and many other applications. Lastly, the approach can be used for first responders to battery-related accidents.

Acknowledgments

Funding was provided from Vehicle Technologies Office of the Energy Efficiency and Renewable Energy Office of the U.S. Department of Energy. This manuscript has been authored by Battelle Energy Alliance, LLC under Contract No. DE-AC07-05ID14517 with the U.S. Department of Energy. The United States Government retains and the publisher, by accepting the article for publication, acknowledges that the United States Government retains a nonexclusive, paid-up, irrevocable, worldwide license to publish or reproduce the published form of this manuscript, or allow others to do so, for United States Government purposes.

References

1. M. Durga Prasad, S. Sathyanarayana, *J. Power Sources*, **19**(1), 67 (1987).
2. A. H. Zimmerman, *IEEE AESS Syst. Mag.*, **19**(2), 19 (2004).
3. K. Yokotani, U.S. Pat. 8,643,332 B2 (2014).
4. A. W. Keates, N. Otani, D. J. Nguyen, N. Matsumura, and P. T. Li, U.S. Pat. 7,795,843 B2 (2010).
5. E. M. Berdichevsky, K. R. Kelty, and S. I. Kohn, U.S. Pat. 7,683,575 B2 (2010).
6. D. A. White, PCT/US2012/045948 (WO 2013009696 A1) (2013).
7. C. McCoy, S. Sriramulu, R. Stringfellow, D. Ofer, and B. Barnett, in *46th Power Sources Conf.,* Orlando, FL (2014), (http://www.camxpower.com/wp-content/uploads/4-6.pdf).
8. C. McCoy, S. Sriramulu, B. Barnett, in *32nd Annual Int. Battery Semin. and Exhib.,* p. 720, Fort Lauderdale, FL, 2015, Curran Associates, Inc., Proceedings.com, (2015).
9. C. H. McCoy, U.S. Pat. Publ. 20140266229 A1 (2014).
10. S. V. Sazhin, E. J. Dufek, K. L. Gering, *ECS Trans*., **73**(1), 161 (2016).
11. S. V. Sazhin, E. J. Dufek, K. L. Gering, *J. Electrochem. Soc*., **164**(1), A6287 (2017).
12. S.V. Sazhin, E.J. Dufek, K.L. Gering, PCT/US2016/062007 (WO 2017/095622 A1) (2017).